https://doi.org/10.1093/brain/awac215 BRAIN 2022: 00; 1–9 | 1

BRAIN REPORT

Recurrent *de novo* mutations in *CLDN5* induce an anion-selective blood–brain barrier and alternating hemiplegia

Yosuke Hashimoto,[1,†] Karine Poirier,[2,†] Nathalie Boddaert,[2,3] Laurence Hubert,[2] Melodie Aubart,[4] Anna Kaminska,[4] Marianne Alison,[5] Isabelle Desguerre,[4] Arnold Munnich[2,4,‡] and Matthew Campbell[1,‡]

[†,‡] **These authors contributed equally to this work.**

Claudin-5 is the most enriched tight junction protein at the blood–brain barrier. Perturbations in its levels of expression have been observed across numerous neurological and neuropsychiatric conditions; however, pathogenic variants in the coding sequence of the gene have never been reported previously. Here, we report the identification of a novel *de novo* mutation (c.178G>A) in the *CLDN5* gene in two unrelated cases of alternating hemiplegia with microcephaly. This mutation (G60R) lies within the first extracellular loop of claudin-5 and based on protein modelling and sequence alignment, we predicted it would modify claudin-5 to become an anion-selective junctional component as opposed to a purely barrier-forming protein.

Generation of stably transfected cell lines expressing wild-type or G60R claudin-5 showed that the tight junctions could still form in the presence of the G60R mutation but that the barrier against small molecules was clearly attenuated and displayed higher Cl^- ion permeability and lower Na^+ permeability.

While this study strongly suggests that *CLDN5* associated alternating hemiplegia is a channelopathy, it is also the first study to identify the conversion of the blood–brain barrier to an anion-selective channel mediated by a dominant acting variant in *CLDN5*.

1 Smurfit Institute of Genetics, Trinity College Dublin, Dublin 2, Ireland
2 INSERM UMR1163, Institut Imagine, Université Paris Cité, F-75015, Paris France
3 Department of Pediatric Radiology, Hospital Necker Enfants Malades, Paris, France
4 Departments of Pediatric Neurology and Medical Genetics, Hospital Necker Enfants Malades, Université Paris Cité, F-75015, Paris France
5 Department of Pediatric Radiology, Hospital Robert Debré, Université Paris Cité, F-75015, Paris France

Correspondence to: Professor Matthew Campbell
Smurfit Institute of Genetics, Trinity College Dublin
Dublin 2, Ireland
E-mail: matthew.campbell@tcd.ie

Correspondence may also be addressed to: Professor Arnold Munnich
INSERM UMR1163, Institut Imagine
Université Paris Cité, F-75015, Paris, France
E-mail: arnold.munnich@inserm.fr

Received March 11, 2022. Revised May 19, 2022. Accepted May 26, 2022. Advance access publication June 17, 2022

Keywords: blood–brain barrier; claudin-5; tight junction; alternating hemiplegia; channelopathy

Abbreviations: ASL = arterial spin labelling; BBB = blood–brain barrier; CBF = cerebral blood flow; HEK = human embryonic kidney

Introduction

The blood–brain barrier (BBB) is critical for maintaining neural homeostasis, strictly regulating the entry and exit of material in the brain.[1] It is now well established that BBB disruption is a common occurrence in a range of neurological and neuropsychiatric conditions, however, the underlying mechanisms that drive this disruption are still not fully resolved.[2] Added to this, identifying novel methods for stabilizing BBB integrity may represent a powerful therapeutic modality for a range of debilitating conditions.[3]

Unique to the BBB are well-evolved endothelial tight junctions, which, as the name suggests, seal the paracellular cleft between two contacting cells.[4] The density of these tight junctions is due in a large part to the presence of high levels of the barrier-forming tight junction protein claudin-5. Indeed, the levels of claudin-5 dominate any other claudin at the BBB and recent single cell RNA-sequencing studies in mice suggest that claudin-5 is amongst the highest expressed protein in cerebrovascular endothelial cells. Claudin-5 is expressed throughout the vasculature of the brain with the highest levels of expression observed in capillaries and small venules.[5]

Claudin-5 is a four-pass transmembrane protein with two extracellular loops that interact homotypically with those of an adjacent cell.[6] These extracellular loops have been shown to have conserved regions typical across numerous claudin species. In fact, it is the amino acid sequence differentials of the extracellular loops that confer unique properties on claudins. For example, claudins-2 and -15 form cation-selective channels[7,8] while claudins-8 and -17 form anion-selective channels.[9,10] Claudin-5 is exclusively a barrier-forming claudin.

It has been shown that inhibition of the barrier-forming function of claudin-5, using neutralizing antibodies, induced convulsions in monkeys.[11] It is also a dosage sensitive gene with heterozygosity probably representing a driving force of BBB disruption observed in 22Q11 deletion syndrome.[12] Added to this, decreases in its levels of expression represents a key pathological feature across a range of conditions including epilepsy, Alzheimer disease, multiple sclerosis and schizophrenia to name a few.[13–15] However, there has never been a report in the literature of variants in the coding sequence of the gene being associated with human disease.

Alternating hemiplegia of childhood is a rare early-onset condition affecting ~1 in 1 million people globally. It is characterized by repeated episodes of transient hemiplegia (lack of motor control on one side of the body), tonic or dystonic attacks (muscle spasms), nystagmus (involuntary eye movement) and choreoathetotic movement (involuntary twitching/writhing). Episodes of quadriplegia can also occur either when a hemiplegia shifts from one side to the other or as an isolated manifestation. Acute episodes are frequently severe and can be followed by cognitive deterioration. Although patients also present with epileptic seizures, the condition is traditionally regarded as being distinct from epilepsy.[16]

Alternating hemiplegia has been occasionally ascribed to pathogenic variants in several ion channel genes including *SCN1A*, *CACNA1A*, *ATP1A3* and *ATP1A2*. In the case of mutations in *ATP1A3* or *ATP1A2*, the mutations lead to reduced activity of Na^+/K^+ ATPase, and affect its ability to efficiently transport ions.[17–19] While alternating hemiplegia is classified as an autosomal dominant condition, almost all cases are as a result of *de novo* mutations.

Here we show that a single, recurrent *de novo* pathogenic variant (c.178G>A) in the *CLDN5* gene converts the tight junction into an anion-selective channel, causing an alternating hemiplegia in two unrelated patients. The concept of the BBB being converted into an anion-selective channel has implications for how we understand hemiplegia. Additionally, considering *CLDN5* associated hemiplegia as a channelopathy opens avenues to therapeutic intervention of this debilitating condition. Notwithstanding the importance of this observation to hemiplegia, its relevance to tight junction and BBB biology also has major implications for our understanding of barrier function and transport mechanisms in the brain in general.

Materials and methods

Full methodology detailing neuroimaging, exome sequencing, homology modelling, plasmid vectors, transfected cells, confocal microscopy, real-time RT-PCR, western blotting and measurement of claudin-5 barrier function are provided in the Supplementary material.

Data availability

All raw data is included in this paper and is publicly available. There are no large datasets associated with the study.

Results

Identification and diagnosis of hemiplegia in two unrelated patients

Patient 1, a girl, was the second child of healthy unrelated parents of Jewish Tunisian ancestry. She was born by caesarean section after a term pregnancy (birthweight 3.310 kg; height 48.5 cm; occipital frontal circumference 33.5 cm). She reportedly held her head aged 3 months, followed with eyes and smiled normally and could sit unaided aged 8 months. She first came to medical attention for recurrent seizures and small head circumference (−2 SD at 2 months). At 8 months, she had three episodes of febrile tonic-clonic seizures of the four limbs, with eye rolling, loss of consciousness, transient left and right post-ictal hemiparesis and vomiting. Inter-ictal EEG was globally slow with neither spikes nor spike waves, suggestive of an encephalitis. EEG records subsequently became asymmetric with poor, slow left background activity. Seizures were controlled by valproate, subsequently replaced with lamotrigine and levetiracetam. She gained height normally but she was overweight (+3 SD) and her head circumference rapidly decelerated (−2 SD at 9 months, −3 SD at 6 years) and stabilized at −3 SD at 12 years. Extensive metabolic workup

detected mildly elevated plasma (3–4 mmol/l) and CSF lactate (3 mmol/l, normal below 2.4) and normal CSF cellularity and immunoglobulins and interferon levels (<2 U/l). Panel screening of reported interferonopathy genes failed to detected any pathogenic variants.

Patient 2, a boy, was the first child of healthy unrelated parents of Asian and European origin. He was born after a full term, uneventful pregnancy and normal delivery (birthweight 4.110 kg; height 52 cm, occipital frontal circumference 36 cm). He thrived normally despite a reported weak sucking while feeding and delayed motor development. He could sit unaided at 11 months, crawl at 14 months, stand at 17 months and walk at 33 months. He first came to medical attention at 30 months for three iterative episodes of febrile and non-febrile hemiplegia and loss of consciousness within 1 month. The recurrent episodes alternatively involved the left- and right-hand side, then generalized and were followed by post-ictal hemiparesis. Two subsequent episodes of prolonged, left hemicorporeal seizures followed by post-ictal right hemiparesis occurred at 34 months and 6½ years, respectively. During this period, inter-ictal EEG tracks showed asymmetric, slowly biphasic and occasionally pseudo-periodic waves on the right temporal and occipital regions without spikes or spike waves. EEG remained asymmetric with low voltage and poor background activity on the same side. Left occipital spikes were also recorded during bouts of seizures at 6½ years. Apart from acute episodes, EEGs were subnormal and never disclosed any epileptiform anomalies. He gained height and weight normally but his head circumference gradually decelerated from 8 months on (–1 SD at 16 months, –2 SD at 27 months) and stabilized close to –2.5 SD at 4 years. Epileptic episodes were controlled by valproate, subsequently replaced with clobazam and stiripentol. Extensive metabolic workup, CSF cellularity, immunoglobulin and interferon levels were unremarkable, and panel sequencing of known epilepsy causing genes failed to detect any pathogenic variants.

Brain calcification and aberrant blood flow patterns are observed in patients with G60R claudin-5 mutations

CT scans of the two patients showed a single calcification in the medial part of the brainstem (Fig. 1A–B, left). In Patient 1, bilateral subcortical calcifications were also observed in the frontal lobes, adjacent to the lateral ventricles (Fig. 1A, right). No other calcifications were observed in Patient 2 (Fig. 1B, right).

In basal conditions, brain MRI of Patient 2 showed a balanced hemispheric cerebral blood flow (CBF, 32 ml/min/100 g of tissue) and a slight, isolated T_2 hyperintensity of the right hippocampus of both patients (Fig. 1C and D, left).

During acute episodes of alternating hemiplegia, arterial spin labelling (ASL) sequences showed a 3-fold contralateral increase of CBF when left hemiplegia was observed, with no cytotoxic oedema (Patient 1: right CBF = 92 ml/min/100 g tissue, left CBF = 25 ml/min/100 g tissue, Fig. 1E). This was also observed in Patient 2 (right CBF = 152 ml/min/100 g, left CBF = 47 ml/min/100 g) and was in stark contrast to the baseline ASL image obtained previously from this patient (Fig. 1H and G, baseline). During a subsequent episode of unilateral (right) hemiplegia, the ASL sequence also revealed a markedly increased CBF in the left hemisphere (right CBF 36 ml/min/100 g, left 143 ml/min/100 g of tissue) (Fig. 1F).

A variant in *CLDN5* associates with hemiplegia

Using exome sequencing, a single base change (c.178G>A) was observed in the *CLDN5* gene of both patients. This variant was located in the coding sequence (p.Gly60Arg) and occurred *de novo* as it was not detected in genomic DNA of their parents (Fig. 2A). This region is highly conserved across species and was predicted to be deleterious using multiple algorithms (Sift, MutationTaster and PolyPhen). It has been hypothesized that charged amino acids in the first extracellular loop domain, especially between β3 and β4 strands, associate with ion selectivity of tight junctions.[19] For example, claudins-8 and -17 have more arginine,[9,10] a positively charged amino acid, in this domain compared to other claudins and function as an anion-selective channel, while barrier-forming claudins like claudins-1, -3 and -5 have less charged amino acids within this domain.[6] In addition, all canonical claudins have small hydrophobic amino acids at position 60 (Fig. 2B) and substituting glycine to cysteine, a hydrophilic amino acid, in claudin-2 at position 60 caused mislocalization of claudin-2, probably due to misfolding.[20]

Sequence alignment and protein modelling suggested that the glycine to arginine substitution would result in creating an ion pathway similar to that observed in claudin-15 (Fig. 2B–D) or causing mislocalization similar to that observed in G6°C claudin-2.

Wild-type and mutant claudin-5 (G60R) localize to the cell surface and at tight junctions

In an effort to explore the effect of the G60R mutation on claudin-5 protein expression, we first generated a stably transfected human embryonic kidney (HEK) cell line expressing wild-type and G60R claudin-5. HEK cells do not have tight junctions and do not constitutively express claudin-5. Fluorescence-activated cell sorting analysis showed stable expression of claudin-5 in both wild-type and mutant states (Fig. 3A), indicating that subcellular localization of this mutant is correct. In addition, claudin-5 was observed to localize to the cell surface and boundaries in both states (Fig. 3B), indicating that the G60R mutant retains the ability for trans-interaction without the assistance of other claudins. No change in claudin-5 transcript (Fig. 3C) or protein (Fig. 3D) was observed in stably transfected HEK cells.

As there was no apparent phenotype in HEK cells expressing G60R claudin-5, we sought to generate a stably transfected cell line that has endogenous tight junctions but no constitutive claudin-5 expression or has endogenous claudin-5. In that regard, we generated stably transfected MDCKII cells and b.End3 cells. MDCKII cells have well-developed tight junction scaffolds, while b.End3 cells do not; however, they are a representative *in vitro* model of the BBB. Both wild-type and G60R claudin-5 were successfully expressed on the cell surface of MDCKII cells (Fig. 3E) and b.End3 cells (Fig. 3F). We also prepared MDCKII cells lowly expressing wild-type claudin-5 and b.End3 cells lacking endogenous claudin-5 to use for functional analysis. The lowly wild-type claudin-5 expressing MDCKII cells showed nearly 3-fold lower mRNA and protein expression levels compared to G60R expressing cells (Fig. 3G and E). The expression of wild-type or G60R claudin-5 changed the expression level of some other major claudins expressed in MDCKII cells (Fig. 3H). The expression of human claudin-5 in b.End3 cells did not change the mRNA level of mouse claudin-5 (Fig. 3I). Compared to HEK293 cells, the protein expression level of G60R claudin-5 G60R was weaker than that of wild-type claudin-5 in both MDCKII and b.End3 cells, indicating that the presence and interaction of other claudins may shorten the half-lives of G60R claudin-5 protein (Fig. 3J). Both wild-type and G60R claudin-5 localized strongly at the tight junction in MDCKII cells. (Fig. 3K) and b.End3 cells (Fig. 3L). The localization of human claudin-5 at the tight junction in b.End3 cells was also confirmed (Fig. 3L).

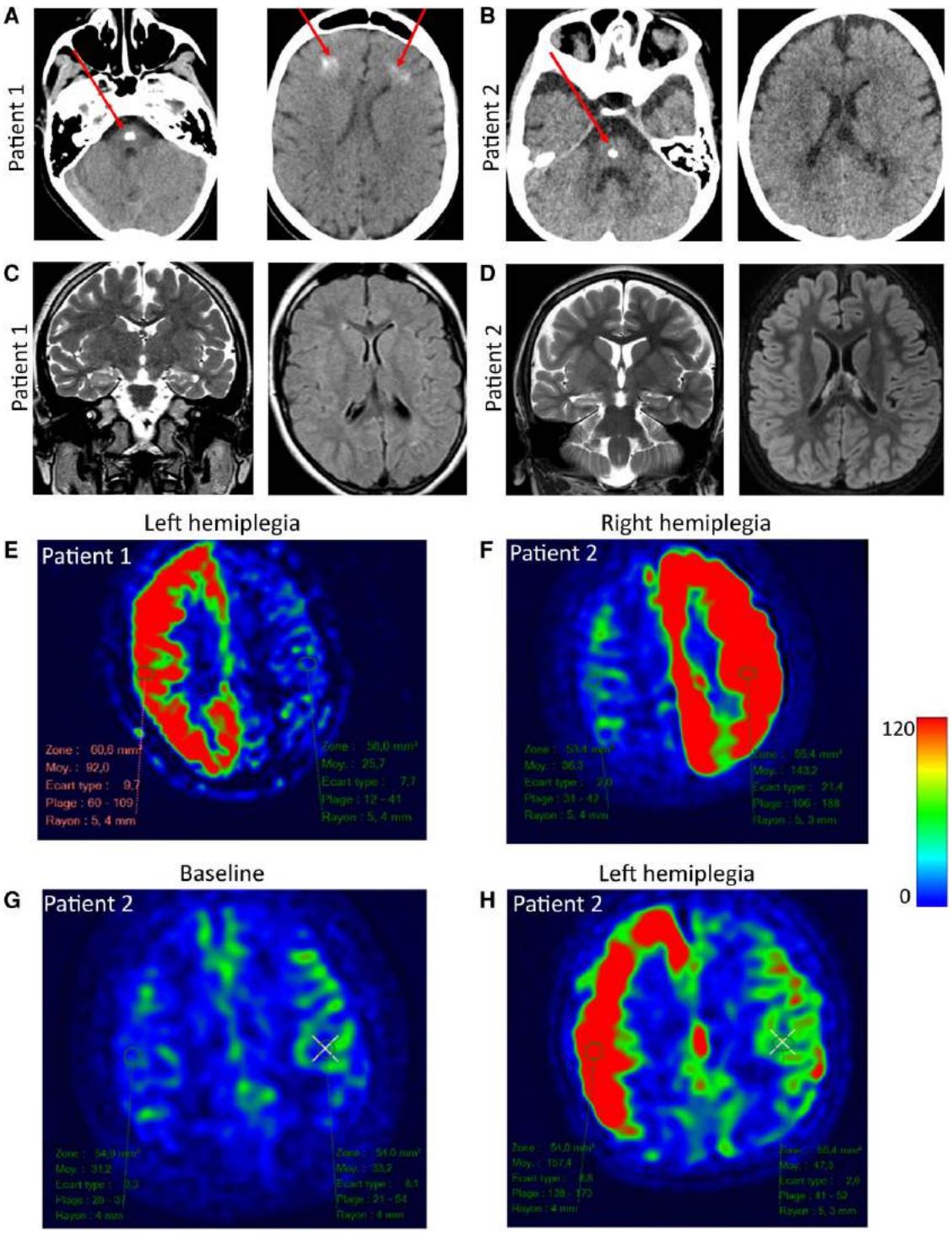

Figure 1 Neuroimaging of patients with hemiplegia. (**A**) Brain CT scan of Patient 1 (aged 6 years). A large calcification is observed in the brainstem in addition to bifrontal, subcortical calcifications in the white matter (red arrow). (**B**) Calcification observed in the brainstem of Patient 2 but no other brain region (red arrow). No cerebellar anomaly, abnormal gyration, corpus callosum anomaly or ventricular dilatation were noted in either patient. (**C**) Brain MRI in basal conditions of Patient 1 (aged 6 years, 6 months) show a moderate, isolated hyperintensity of the right hippocampus with no abnormal gyration or ventricular dilatation on axial FLAIR sequence. (**D**) Similar findings were observed in Patient 2. (**E**) Brain MRI during episodes of alternating hemiplegia in Patient 1. ASL sequence of Patient 1 aged 15 years during an episode of left hemiplegia. Note the unilateral increase of CBF. (**F**) ASL sequence of Patient 2 aged 4.5 years during an episode of right hemiplegia. (**G**) ASL sequence in Patient 2 in basal conditions and (**H**) ASL sequence in Patient 2 aged 1 year, 6/12 during a subsequent episode of left hemiplegia.

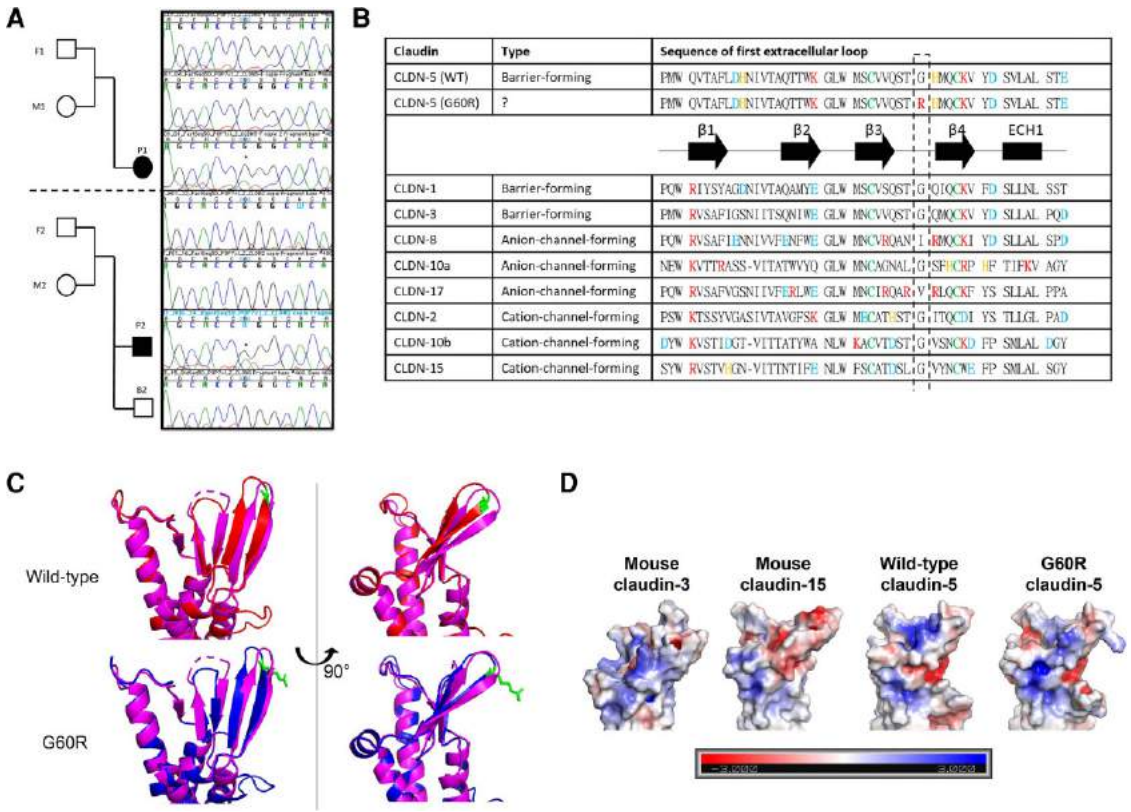

Claudin	Type	Sequence of first extracellular loop
CLDN-5 (WT)	Barrier-forming	PMW QVTAFLDRNIVTAQTTWK GLW MSCVVQST G QMQCKV YD SVLAL STE
CLDN-5 (G60R)	?	PMW QVTAFLDRNIVTAQTTWK GLW MSCVVQST R QMQCKV YD SVLAL STE
		β1 β2 β3 β4 ECH1
CLDN-1	Barrier-forming	PQW RIYSYAGDNIVTAQAMYE GLW MSCVSQST G QIQCKV FD SLLNL SST
CLDN-3	Barrier-forming	PMW RVSAFIGSNIITSQNIWE GLW MNCVVQST G QMQCKV YD SLLAL PQD
CLDN-8	Anion-channel-forming	PQW RVSAFIENNIVVFENFWE GLW MNCVRQAN I KMQCKI YD SLLAL SPD
CLDN-10a	Anion-channel-forming	NEW KVTTRASS-VITATWVYQ GLW MNCAGNAL G SFHCRP HF TIFKV AGY
CLDN-17	Anion-channel-forming	PQW RVSAFVGSNIIVFERLWE GLW MNCIRQAR V RLQCKF YS SLLAL PPA
CLDN-2	Cation-channel-forming	PSW KTSSYVGASIVTAVGFSK GLW MECATNST G ITQCDI YS TLLGL PAD
CLDN-10b	Cation-channel-forming	DYW KVSTIDGT-VITTATYWA NLW KACVTDST G VSNCKD FP SMLAL DGY
CLDN-15	Cation-channel-forming	SYW RVSTVNGN-VITTNTIFE NLW FSCATDSL G VYNCWE FP SMLAL SGY

Figure 2 *CLDN5* variant and protein modelling. (**A**) Trio pedigree of parents and children diagnosed with hemiplegia. Sanger sequencing chromatograms showing (c.178G>A) variant in the *CLDN5* gene. (**B**) Sequence alignment in the first extracellular loop of representative human claudins with predicted secondary structure of CLDNs. Three types of representative CLDN are chosen: barrier-forming CLDNs (claudin-1, -3), anion-selective channel-forming CLDNs (CLDN-8, -10a, -17) and cation-selective channel-forming CLDNs (CLDN-2, −10b, −15). The secondary structure of CLDNs is shown with α-helices and β-strands represented by cylinders and arrows, respectively. Blue = negatively charged amino acids; red = positively charged amino acids; orange = histidine; green = conserved cystine. (**C**) Predicted structure of wild-type (WT) (red) and variant CLDN-5 (blue) based on the homology of mouse CLDN-15 (pink). Amino acid position at 60 is highlighted in green. (**D**) The electrostatic potentials (units kT/*e*) on the surface of mouse CLDN-3, mouse CLDN-15, wild-type or G60R CLDN-5 are shown.

Mutant claudin-5 (G60R) creates anion-selective permeability and a weakened barrier against small molecules

Functional analysis of MDCKII and b.End3 tight junctions showed that expression of either wild-type or G60R claudin-5 induced a significant increase in trans-epithelial/endothelial electrical resistance (TEER) (Fig. 4A). The wild-type claudin-5 increased TEER compared to G60R claudin-5 in both MDCKII and b.End3 cells. Intriguingly, the TEER of G60R claudin-5 expressing MDCKII cells was comparable to that of wild-type low cells, suggesting the barrier-forming ability of G60R claudin-5 is ∼3-fold weaker than that of wild-type claudin-5. When we applied a 2:1 NaCl gradient across G60R claudin-5 expressing cells, they showed significantly lower dilution potential compared to wild-type claudin-5 expressing cells (Fig. 4B), indicating that the ratio between the permeability of Na^+ and that of Cl^- (P_{Na}/P_{Cl}) was decreased in G60R claudin-5 expressing cells. The absolute permeabilities of Na^+ and Cl^- were calculated using the Goldman–Hodgkin–Katz equation and the Kimizuka–Koketsu equation (Fig. 4C). By expression of wild-type claudin-5, both Na^+ and Cl^- permeabilities were decreased in a dose-dependent manner in MDCKII cells. However, expression of G60R claudin-5 only slightly attenuated Cl^- permeability while it strongly attenuated Na^+ permeability in both MDCKII and b.End3 cells. Compared to lowly wild-type claudin-5 expressing MDCKII cells, G60R expressing MDCKII cells showed lower Na^+ permeability and higher Cl^- permeability, indicating that the electrical barrier created by G60R prevents cation permeation to create an exclusively anion-selective channel.

As we had predicted that G60R claudin-5 would induce an anion-selective pore at the tight junction, we conducted size-selective flux assays of fluorescent tracer molecules across the stably transfected MDCKII and b.End3 monolayers. Indeed, G60R claudin-5 expressing cells displayed enhanced flux of sodium fluorescein (377 Da) compared to wild-type claudin-5 expressing cells, (Fig. 4D), suggesting that the barrier formed by G60R claudin-5 is more permissive against the diffusion of small molecular-weight molecules compared to the barrier formed by wild-type claudin-5. Enhanced permeation of FITC-Dextran (4 kDa) was also observed in G60R expressing b.End3 cells but not MDCKII cells (Fig. 4E).

Discussion

Several human diseases have been ascribed to pathogenic variants in members of the *CLDN*-family genes. These include variants associating with conditions such as ichthyosis alopecia and sclerosing cholangitis (*CLDN1*), hypercalciuria (CLDN2), autosomal recessive deafness (*CLDN9* and *CLDN14*), HELIX syndrome (*CLDN10*), tubular hypomagnesaemia (*CLDN16* and *CLDN19*) and hypomyelinating leukodystrophy (*CLDN11*).[21–25] Our study is the first report of a variant in the coding

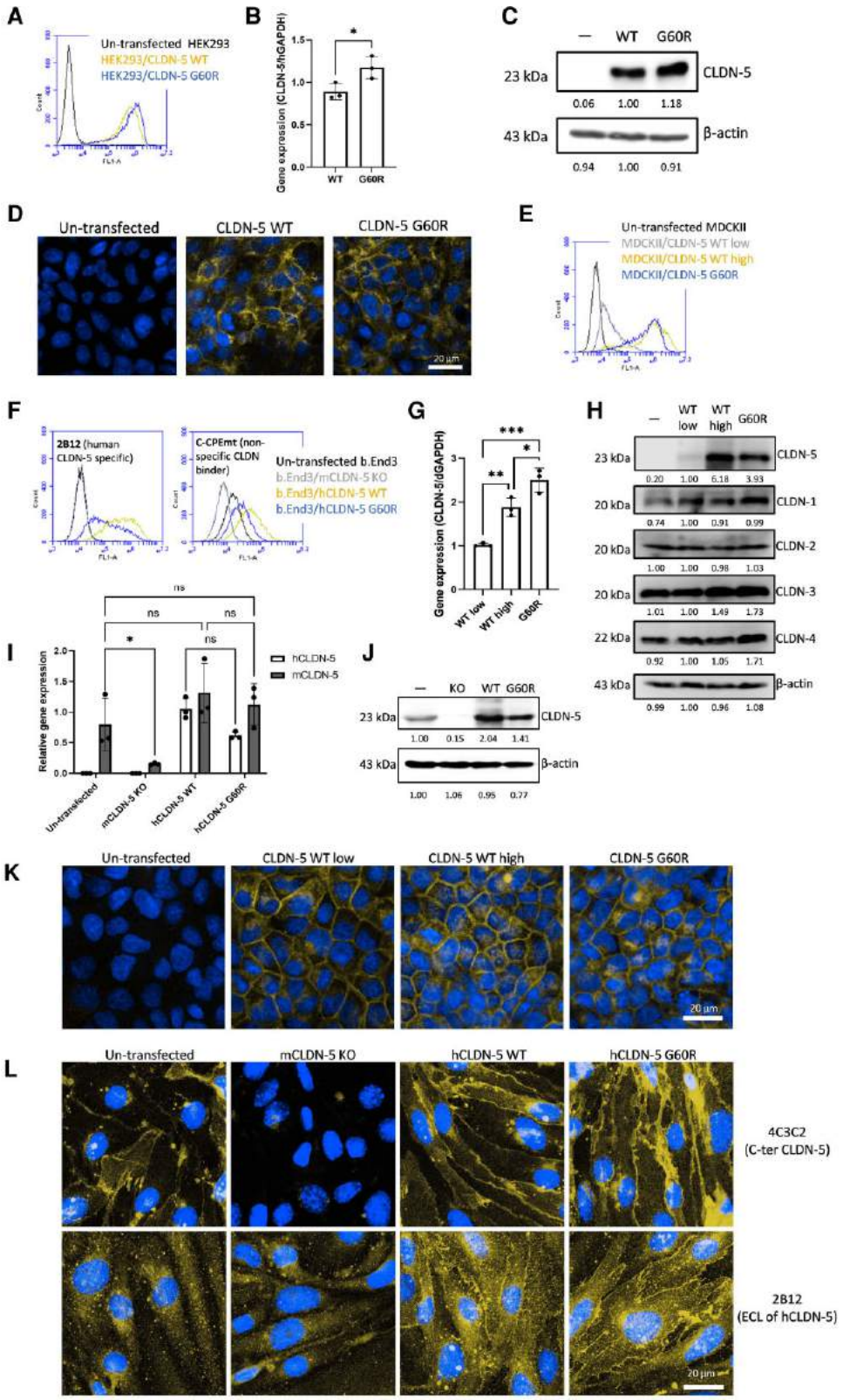

Figure 3 The effect of G60R mutation on CLDN-5 expression and localization in CLDN-null cells. Stable transfectants of HEK293 cells (CLDN-null cells) (**A**–**D**), MDCKII cells (CLDN-competent cells) (**E**, **G**, **H** and **K**) or b.End3 cells (mouse brain endothelial cell line) (**F**, **I**, **J** and **L**) expressing CLDN-5 wild-type (WT) or G60R were established. (**A**, **E** and **F**) Cell-surface expression of CLDN-5 in HEK293, MDCKII and b.End3 transfectants respectively was analysed using an antibody recognizing the extracellular domain of CLDN-5 or non-specific CLDN-binding molecule (C-CPEmt). (**C**, **G** and **I**) The transcript levels of claudin-5 and (**D**, **H** and **J**) protein levels of CLDN-5 and other major CLDNs in transfectants. (**B**, **K** and **L**) Subcellular localization of CLDN-5 in transfectants was checked by confocal microscopy. Green = CLDN-5, blue = nuclei. Scale bar = 20 μm.

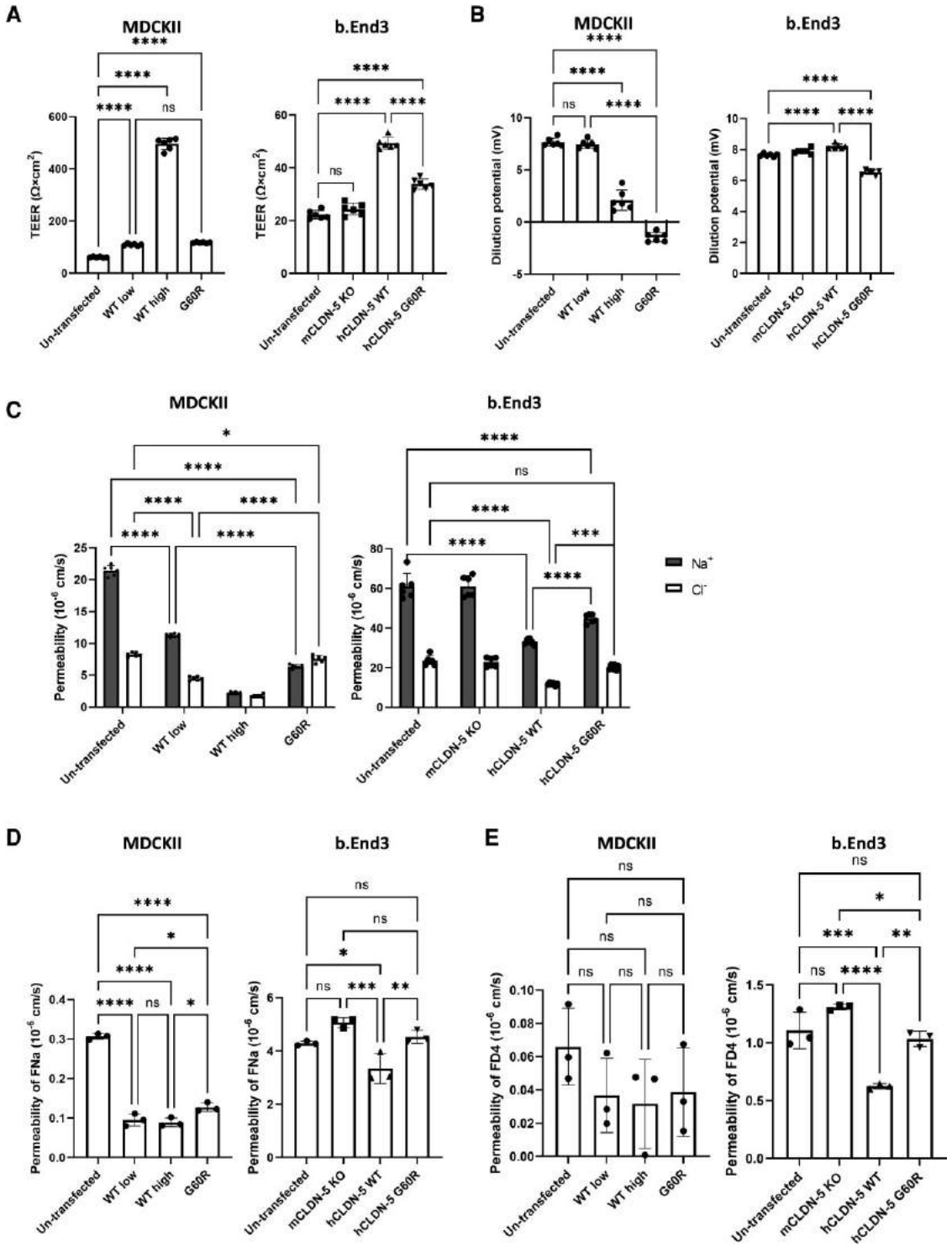

Figure 4 The effect of G60R mutation on barrier-forming function of CLDN-5. Untransfected cells or cells expressing CLDN-5 wild-type (WT) low and wild-type high or G60R were cultured on cell culture inserts for 5 days (MDCKII cells) or 8 days (b.End3 cells) to prepare a well-developed monolayer. (**A**) TEER and (**B**) the dilution potential of NaCl were measured and (**C**) absolute Na^+ and Cl^- permeabilities were calculated. Values represent the mean ± SD. ($n = 6$). (**D**) The permeability of sodium fluorescein (377 Da) and (**E**) 4 kDa of fluorescence-conjugated dextran (FD4) across the monolayers were measured. Values represent the mean ± SD ($n = 3$).

region of the *CLDN5* gene associated with a neurological condition. As described, claudin-5 is a critical tight junction component of the BBB and its levels are essential in maintaining the correct barrier functioning of the microvasculature of the brain. Our study, however, highlights the potential for variants in *CLDN5* to convert the tight junction from a barrier to an anion-selective channel, which is probably a key driver of the disease in this form of alternating hemiplegia.

Key amino acids associated with intramolecular interaction and homophilic *cis*-interaction of claudin-5 were predicted by an *in silico* study but G60 is not involved with these interactions. G60 is located

in a flexible loop between in β3 and β4 strands and the flexible loop is predicted to be located in the middle of the pore centre created by *cis*- and *trans*-interacting claudin tetramers. In claudin-15, mutation of D55, also located in the middle of the pore centre, to a neutral amino acid (D55N) decreased the cation selectivity and mutation of D55 to a positively charged amino acid (D55K) and converted its ion selectivity.[26] D55, corresponding to Q57 of claudin-5 (Fig. 2C), has more impact on the charge-selectivity of claudin-15 compared to other charged amino acids in other domains because the region of D55 facilitates the main interacting site for ions. Therefore, potentially other undiscovered mutations that change the amino acids in the flexible loop of claudin-5 (V56 to H61) to charged amino acids may show a similar effect/symptoms. The expression level of claudin-5 clearly inversely correlates with the prevalence and severity of psychiatric disorders and epilepsy.[12,13] We estimate that the barrier-forming ability of G60R claudin-5 is <30% of that observed in wild-type claudin-5. However, the symptoms in carriers of the G60R mutation may be different from holders with mutations that disrupt *cis*- or *trans*-interaction of claudin-5 or induce mislocalization of claudin-5 because G60R completely changes the ion preference of claudin-5.

The brainstem calcification we observed in the two patients is reminiscent of and closely similar to that observed in patients carrying biallelic mutations in occludin[27] or junctional adhesion molecule 2 (JAM2), another tight junction protein of the BBB.[28] Both occludin and JAM2 are mainly expressed in endothelial cells in the CNS.[5] The contribution of JAM2 to the integrity of the tight junction in the BBB may be minor[29] but occludin is known to enhance the complexity of tight junction strands and the knockdown of occludin attenuated TEER of a brain endothelial cell line.[30] Indeed, levels of occludin are also frequently perturbed in a range of neurological conditions and it is likely that decreases in its levels at the BBB tight junction contribute to selective ion flux from blood to brain in a manner that will drive pathology. On the other hand, the transient contralateral increase of CBF observed in patients with variant *CLDN5* during the acute episodes of hemiplegia is reminiscent of cases of alternating hemiplegia ascribed to pathogenic variants in another ion channel gene, *ATP1A3*. However, the ASL pattern reported here could not be ascribed to pre- or post-ictal events as no seizure concomitant with the transient episodes of hemiplegia were noted. One can hypothesize that the conversion of the wild-type tight junction protein into a channel-forming mutant claudin-5 protein lowered seizure threshold by disturbing brain microenvironment and transiently triggered neuronal injury similar to the stroke-like episodes observed in Leigh syndrome. It is plausible that when one hemisphere requires vasodilation of contiguous vessels to supply oxygen and ATP, it can compromise the contralateral hemisphere. Indeed, to our knowledge this is also the first ASL evidence of a major contralateral increase of CBF observed in alternating hemiplegia. Beyond its relevance to hemiplegia, the concept of the BBB converting to an anion-selective channel via changes to the extracellular domain of claudin-5 represents a paradigm shift in how we view the BBB.

Acknowledgements

The authors would like to thank Dr Claude Besmond for contributions to the study.

Funding

This work was supported by grants from Science Foundation Ireland (SFI), (12/YI/B2614 and 11/PI/1080), The Irish Research Council (IRC) and by a research grant from SFI under grant number 16/RC/3948 and co-funded under the European Regional Development fund by FutureNeuro industry partners. The Campbell laboratory is also supported by a European Research Council (ERC) grant, 'Retina-Rhythm' (864522). Y.H. is supported by the Japan Society for the Promotion of Science (JSPS) as an overseas research fellow.

Competing interests

The authors report no competing interests.

Supplementary material

Supplementary material is available at *Brain* online.

References

1. Abbott NJ, Patabendige AAK, Dolman DEM, *et al*. Structure and function of the blood-brain barrier. *Neurobiol Dis*. 2010;37:13–25.
2. Greene C, Hanley N, Campbell M. Claudin-5: gatekeeper of neurological function. *Fluids Barriers CNS*. 2019;16:3.
3. Martin M, Vermeiren S, Bostaille N, *et al*. Engineered Wnt ligands enable blood-brain barrier repair in neurological disorders. *Science*. 2022;375:eabm4459.
4. Hudson N, Campbell M. Tight junctions of the neurovascular unit. *Front Mol Neurosci*. 2021;14:752781.
5. Vanlandewijck M, He L, Mäe MA, *et al*. A molecular atlas of cell types and zonation in the brain vasculature. *Nature*. 2018;554:475–480.
6. Piehl C, Piontek J, Cording J, Wolburg H, Blasig IE. Participation of the second extracellular loop of claudin-5 in paracellular tightening against ions, small and large molecules. *Cell Mol Life Sci*. 2010;67:2131–2140.
7. Luettig J, Rosenthal R, Barmeyer C, Schulzke JD. Claudin-2 as a mediator of leaky gut barrier during intestinal inflammation. *Tissue Barriers*. 2015;3(1-2):e977176.
8. Alberini G, Benfenati F, Maragliano L. Molecular dynamics simulations of ion selectivity in a claudin-15 paracellular channel. *J Phys Chem B*. 2018;122:10783–10792.
9. Hou J, Renigunta A, Yang J, Waldegger S. Claudin-4 forms paracellular chloride channel in the kidney and requires claudin-8 for tight junction localization. *Proc Natl Acad Sci U S A*. 2010;107:18010–5.
10. Conrad MP, Piontek J, Günzel D, Fromm M, Krug SM. Molecular basis of claudin-17 anion selectivity. *Cell Mol Life Sci*. 2016;73:185–200.
11. Tachibana K, Hashimoto Y, Shirakura K, *et al*. Safety and efficacy of an anti-claudin-5 monoclonal antibody to increase blood-brain barrier permeability for drug delivery to the brain in a non-human primate. *J Control Release*. 2021;336:105–111.
12. Greene C, Kealy J, Humphries MM, *et al*. Dose-dependent expression of claudin-5 is a modifying factor in schizophrenia. *Mol Psychiatry*. 2018;23:2156–2166.
13. Greene C, Hanley N, Reschke CR, *et al*. Microvascular stabilization via blood-brain barrier regulation prevents seizure activity. *Nat Commun*. 2022;13:2003.
14. Hüls A, Robins C, Conneely KN, *et al*. Brain DNA methylation patterns in CLDN5 associated with cognitive decline. *Biol Psychiatry*. 2022;91:389–398.
15. van Horssen J, Brink BP, de Vries HE, van der Valk P, Bø L. The blood-brain barrier in cortical multiple sclerosis lesions. *J Neuropathol Exp Neurol*. 2007;66:321–328.
16. Uchitel J, Helseth A, Prange L, *et al*. The epileptology of alternating hemiplegia of childhood. *Neurology*. 2019;93:e1248–e1259.

17. Bassi MT, Bresolin N, Tonelli A, *et al*. A novel mutation in the ATP1A2 gene causes alternating hemiplegia of childhood. *J Med Genet*. 2004;41:621–628.
18. Heinzen EL, Swoboda KJ, Hitomi Y, *et al*. De novo mutations in ATP1A3 cause alternating hemiplegia of childhood. *Nat Genet*. 2012; 44:1030–1034.
19. Rosenthal R, Günzel D, Krug SM, Schulzke JD, Fromm M, Yu AS. Claudin-2-mediated cation and water transport share a common pore. *Acta Physiol (Oxf)*. 2017;219:521–536.
20. Li J, Zhuo M, Pei L, Rajagopal M, Yu ASL. Comprehensive cysteine-scanning mutagenesis reveals claudin-2 pore-lining residues with different intrapore locations. *J Biol Chem*. 2014; 289:6475–6484.
21. Askari M, Karamzadeh R, Ansari-Pour N, *et al*. Identification of a missense variant in CLDN2 in obstructive azoospermia. *J Hum Genet*. 2019;64:1023–1032.
22. Sineni CJ, Yildirim-Baylan M, Guo S, *et al*. A truncating CLDN9 variant is associated with autosomal recessive nonsyndromic hearing loss. *Hum Genet*. 2019;138:1071–1075.
23. Wilcox ER, Burton QL, Naz S, *et al*. Mutations in the gene encoding tight junction claudin-14 cause autosomal recessive deafness DFNB29. *Cell*. 2001;104:165–172.
24. Hadj-Rabia S, Brideau G, Al-Sarraj Y, *et al*. Multiplex epithelium dysfunction due to CLDN10 mutation: the HELIX syndrome. *Genet Med*. 2018;20:190–201.
25. Riedhammer KM, Stockler S, Ploski R, *et al*. De novo stop-loss variants in CLDN11 cause hypomyelinating leukodystrophy. *Brain*. 2021;144:411–419.
26. Samanta P, Wang Y, Fuladi S, *et al*. Molecular determination of claudin-15 organization and channel selectivity. *J Gen Physiol*. 2018;150:949–968.
27. O'Driscoll MC, Daly SB, Urquhart JE, *et al*. Recessive mutations in the gene encoding the tight junction protein occludin cause band-like calcification with simplified gyration and polymicrogyria. *Am J Hum Genet*. 2010;87:354–364.
28. Cen Z, Chen Y, Chen S, *et al*. Biallelic loss-of-function mutations in JAM2 cause primary familial brain calcification. *Brain*. 2020; 143:491–502.
29. Tietz S, Périnat T, Greene G, *et al*. Lack of junctional adhesion molecule (JAM)-B ameliorates experimental autoimmune encephalomyelitis. *Brain Behav Immun*. 2018;73:3–20.
30. Saito AC, Higashi T, Fukazawa Y, *et al*. Occludin and tricellulin facilitate formation of anastomosing tight-junction strand network to improve barrier function. *Mol Biol Cell*. 2021;32:722–738.